



Effects of sheet and rill erosion on soil aggregates and organic carbon losses for a Mollisol hillslope under rainfall simulation

Yiliang Jiang^{1,2} · Fenli Zheng^{1,2}  · Leilei Wen^{2,3} · Hai-ou Shen^{2,3}

Received: 17 March 2017 / Accepted: 22 May 2018
© Springer-Verlag GmbH Germany, part of Springer Nature 2018

Abstract

Purpose Characterizations of soil aggregates and soil organic carbon (SOC) losses affected by different water erosion patterns at the hillslope scale are poorly understood. Therefore, the objective of this study was to quantify how sheet and rill erosion affect soil aggregates and soil organic carbon losses for a Mollisol hillslope in Northeast China under indoor simulated rainfall.

Materials and methods The soil used in this study was a Mollisol (USDA Taxonomy), collected from a maize field (0–20 cm depth) in Northeast China. A soil pan with dimensions 8 m long, 1.5 m wide and 0.6 m deep was subjected to rainfall intensities of 50 and 100 mm h⁻¹. The experimental treatments included sheet erosion dominated (SED) and rill erosion dominated (RED) treatments. Runoff with sediment samples was collected during each experimental run, and then the samples were separated into six aggregate fractions (0–0.25, 0.25–0.5, 0.5–1, 1–2, 2–5, > 5 mm) to determine the soil aggregate and SOC losses.

Results and discussion At rainfall intensities of 50 and 100 mm h⁻¹, soil losses from the RED treatment were 1.4 and 3.5 times higher than those from the SED treatment, and SOC losses were 1.7 and 3.8 times greater than those from the SED treatment, respectively. However, the SOC enrichment ratio in sediment from the SED treatment was 1.15 on average and higher than that from the RED treatment. Furthermore, the loss of < 0.25 mm aggregates occupied 41.1 to 73.1% of the total sediment aggregates for the SED treatment, whereas the loss of > 0.25 mm aggregates occupied 53.2 to 67.3% of the total sediment aggregates for the RED treatment. For the organic carbon loss among the six aggregate fractions, the loss of 0–0.25 mm aggregate organic carbon dominated for both treatments. When rainfall intensity increased from 50 to 100 mm h⁻¹, aggregate organic carbon loss increased from 1.04 to 5.87 times for six aggregate fractions under the SED treatment, whereas the loss increased from 3.82 to 27.84 times for six aggregate fractions under the RED treatment.

Conclusions This study highlights the effects of sheet and rill erosion on soil and carbon losses at the hillslope scale, and further study should quantify the effects of erosion patterns on SOC loss at a larger scale to accurately estimate agricultural ecosystem carbon flux.

Keywords Enrichment ratio · Mollisol of Northeast China · Rill erosion · Sheet erosion · Soil aggregate · Soil organic carbon

Responsible editor: Nikolaus Kuhn

✉ Fenli Zheng
flzh@ms.iswc.ac.cn

¹ Institute of Soil and Water Conservation, State Key Laboratory of Soil Erosion and Dryland Farming in the Loess Plateau, Northwest A & F University, Yangling, Shaanxi 712100, People's Republic of China

² Institute of Soil and Water Conservation, CAS & MWR, Yangling, Shaanxi 712100, People's Republic of China

³ College of Resources and Environment, Northwest A & F University, Yangling, Shaanxi 712100, People's Republic of China

1 Introduction

Soil erosion significantly affects the global carbon (C) cycle in terrestrial ecosystems (Stallard 1998; Lal 2003; Van Oost et al. 2007; Kuhn et al. 2009). Erosion-induced C loss generates considerable interests because this loss is one part of the “missing sink” of the unbalanced global C budget (Tans et al. 1990; Schimel et al. 2001). Identification of unknown C sinks is important for developing strategies for mitigating potential climate change (Lal 2003; Liu et al., 2016). During the past decades, researchers have attempted to quantify erosion-induced loss of soil organic carbon (SOC) in various environments. Rozanov et al. (1993) observed that the world soils lost

humus (58% C) at a rate of 25.3 Tg year⁻¹ since agriculture began 10,000 years ago, 300 Tg year⁻¹ in the past 300 years and 760 Tg year⁻¹ in the last 50 years. Previous studies estimated the current rate of SOC loss by erosion was to be 4.0–6.0 Tg C per year assuming a sediment delivery ratio of 10% and SOC content of 2–3% (Lal 2003). Given the intense interest in assessing erosional SOC loss and the variation among studies, improving the qualitative understanding of the principal processes and factors that affect the rate and magnitude of SOC loss within soils and terrestrial ecosystems is important. Additionally, in the current research, mostly attention is concentrated on sheet erosion-induced SOC loss, but there is little information on rill erosion-induced SOC loss.

Soil aggregation is perceived as an indicator of soil stability and erodibility (Sutherland et al. 1996; Six et al. 2000; Morgan 2005; Zhang et al., 2006a, b). Properties related to soil matrix aggregate stability such as organic content, bulk density and dispersion ratio are also related to soil erodibility (Young and Onstad 1982). In the process of soil erosion, which is affected by raindrop impact and agricultural practices, the explosion of dry aggregates after moistening and mechanical disturbance, among other factors, cause aggregates to lose stability and break into lighter and smaller fractions (Le Bissonnais and Arrouays 1997; Lal 2003). Eroded aggregate size distribution varies during the erosion process at different eroding landform positions (Armstrong and Stein 1996). Additionally, soil aggregates are important in the protection of SOC against rapid decomposition by soil microbes (Tisdall and Oades 1982). The destruction of soil aggregates releases the cementing organic carbon that was previously encapsulated within the aggregates (Polyakov and Lal 2004). With overland flow, soil aggregates and SOC are transported away from eroded soil landscapes. However, the SOC dynamics in soil aggregation and disaggregation during soil detachment, transport and deposition processes are far less well understood (Kuhn et al. 2009; Nadeu et al. 2011).

Most studies show that the selective transport of overland flow results in the enrichment of the eroded sediment with labile SOC (Tiessen et al., 1982; Bajracharya et al. 2000; Lal 2003). Generally, the enrichment ratio (ER) of SOC in the sediment, defined as the ratio of organic carbon content in eroded sediment to that of the tested soil organic carbon, is > 1 (Schietecatte et al. 2008b). Based on a simulated study, Polyakov and Lal (2004) showed that the ER of SOC for sediment leaving the erosional portion of the slope is smaller than that from the depositional portions of the slope. Moreover, researchers have investigated the factors affecting SOC loss by water erosion. For example, Foster and Wischmeier (1974) noted that soil properties, rainfall intensity (duration), topography, surface cover and soil wetness influence SOC loss. In general, the magnitude of SOC transport in runoff water is greater from bare fallow plots than that from plots with vegetal cover (Lal 1976; Lowrance and Richard

1988; Jin et al. 2009), and SOC loss induced by erosion on sloping land may be several times higher than that on flat land. Several studies indicate that conservation tillage practices reduce losses of soil and SOC (Kisic et al. 2002; Puustinen et al. 2005). Maïga-Yaleu et al. (2013) noted that the formation of loose and sandy crusts increases SOC protection from water erosion, which in turn may improve SOC stabilization and associated soil functions. Wang et al. (2014) found that the erosion-induced breakdown of aggregates and the redistribution of aggregate associated SOC lead to an increase in macro-aggregation and macro-aggregate associated C content at the depositional site. The cited research results indicate that because of the above factors, water erosion affects SOC dynamics. However, there are still unknown factors affecting the erosion process and SOC loss. For example, the mechanisms of SOC loss in different water erosion processes, such as splash, sheet, and rill erosion, remain poorly understood. Moreover, erosion processes affecting SOC are not yet modelled in an optimal way, and no good parameterization describes the internal dynamics (Starr et al. 2000; Polyakov and Lal 2004). Consequently, the effects of soil erosion on C dynamics must be assessed objectively and quantitatively, and the discrepancy comparison of soil aggregate breakdown and SOC loss mechanisms in different water erosion processes remains to be quantified.

The Mollisol region of Northeast China (43–50°N, 124–127°E) occupies an area of 5.96 million hectares. With an undulating landscape, concentrated rainfall in the summer and bare soil surface without residue cover under conventional management cause serious rill erosion (Cheng et al. 2010). Moreover, rill and gully erosion are also principal erosion patterns in the Mollisol region. The national survey indicated the number of erosion gullies was approximately 0.25 million, and the destroyed cultivated land area covered approximately 0.48 million hectares in the Mollisol region of Northeast China (MWR et al. 2010). However, current studies on Mollisol erosion mechanisms, particularly for rill and gully erosion mechanisms, remain relatively weak. The non-selective sediment transport during rill erosion is different from sheet erosion, which is selective sediment transport. Currently, SOC loss induced by rill erosion is unknown. Thus, further exploration of the inherent mechanisms of the SOC loss under sheet erosion dominated and rill erosion dominated is necessary. Therefore, the specific objectives of this study were (a) to investigate the characteristics of sheet and rill erosion, (b) to compare soil aggregate loss processes between sheet erosion dominated and rill erosion dominated treatments, and (c) to identify differences of the SOC and aggregate organic carbon losses between sheet and rill erosion. The results from this study improve the understanding of how sheet erosion and rill erosion influence soil aggregates and SOC losses and reveal SOC loss mechanisms for different water erosion patterns.

2 Materials and methods

2.1 Soil properties and experimental setup

The soil used in the experiment was collected from the upper 20 cm of the plough layer in a maize field near Liujia Town (44°43'N, 126°11'E), Yushu City, Jilin Province, which is the centre region of Northeast China. The soil is a silt loam soil and classified as a Mollisol (USDA Taxonomy), with a soil bulk density of 1.20 Mg m⁻³ and with 20.3% clay (< 2 μm), 76.4% silt (2–50 μm) and 3.3% sand (> 50 μm) content. The pH in water was 5.92, measured with a 1:2.5 solid-to-water ratio on a weight basis. The soil contained 23.8 g kg⁻¹ soil organic matter, 18.1 mg kg⁻¹ NO₃-N, 16.0 mg kg⁻¹ NH₄-N and 1.5 mg kg⁻¹ PO₄-P. Before the experiment, the soil was air dried to a moisture content of approximately 4% and then broken into sub-angular blocky clods less than 4 cm in size, but was not sieved and ground to preserve the in situ soil aggregation fabric.

The simulated experiments were conducted in the Rainfall Simulation Laboratory of the State Key Laboratory of Soil Erosion and Dryland Farming on the Loess Plateau, Yangling City, China. A rainfall simulator system with a side sprinkler was used to apply rainfall and the rainfall simulator could be set to any selected rainfall intensity, ranging from 20 to 300 mm h⁻¹, by adjusting water pressure and spray nozzle size. The nozzles were approximately 16 m above the ground surface for the rainfall simulator. The simulated rainfall had uniformity above 90% and was similar to natural rainfall in both raindrop size distribution and kinetic energy (Zhou et al. 2000). The soil pan was 8 m long, 1.5 m wide and 0.6 m deep, and runoff collecting devices were installed at the outlet. The bottom of the soil pan was equipped with 128 drainage holes with a diameter of 2 cm. A 10-cm thick layer of sand was packed at the bottom of the soil pan, which allowed free drainage of excess water. Then layers over the sand were divided into a sticky loess layer (simulating the plough pan) with a depth of 20 cm and a Mollisol layer (simulating the tilth layer) with a depth of 20 cm. The bulk densities for the sticky loess layer and the Mollisol layer were 1.35 and 1.20 g cm⁻³, respectively. Additional details about the packing process of the soil pan are found in An et al. (2012).

2.2 Experimental design and procedures

The experimental design included two treatments: sheet erosion dominated and rill erosion dominated. The top 20 cm of soil in the soil pan for the sheet erosion dominated (SED) treatment was ploughed each time before the experiment. After ploughing, the soil pan was allowed to settle for 2 days, and then the soil surface was harrowed flat for the treatment of SED. For the rill erosion dominated (RED) treatment, an initial channel 2.00 m long and 0.10 m deep and 0.10 m wide was built in the centre of the soil pan, which was located at 5–7 m

slope length of the soil pan (Wei and Xiao, 2005; MWR et al. 2010; Wang et al. 2011). Except for building the rill channel in the soil pan for the RED treatment, other treatment preparation of the soil pan was the same as that for the SED treatment.

In the Mollisol region of Northeast China, the gradient of the hillslope land is generally 1–8° (Zhang et al., 2006a, b), and sometimes it exceeds 10°, where rill erosion frequently occurs. Therefore, 10° was determined as the experimental slope gradient representing the typical slope gradient on which severe soil erosion occurred. According to the annual precipitation (500–700 mm), particularly the record of erosive rainfall events with high rainfall intensity ($I_5 = 1.85 \text{ mm min}^{-1}$, and $I_{15} \geq 0.87 \text{ mm min}^{-1}$) and short duration (40–70% of the total erosive rainstorms last less than 1 h), in the typical Mollisol region of Northeast China, the rainfall intensity in this study was set to 50 and 100 mm h⁻¹ (0.83 and 1.67 mm min⁻¹), respectively.

Before the rainfall simulation experiment, a pre-rain with intensity of 25 mm h⁻¹ was performed on the soil pan for approximately 40 min, and then, the soil pan was allowed to saturate slowly for 24 h. The soil moisture content was measured before each experiment and maintained at 28.6–29.7%. After calibrating the rainfall intensity and maintaining the error below 5%, the simulated rainfall experiment was conducted for the duration of 100 min. Each treatment was repeated twice.

2.3 Experimental measurements

For each treatment, two sets of runoff samples with sediment were collected to investigate the sediment and SOC transport and to analyse the sediment aggregate redistribution and aggregate organic carbon. The first set of runoff samples with sediment was collected during rainfall simulation from the outlet of the soil pan at 5 min intervals using 15 L buckets, and each sample volume was approximately 4–6 L. To avoid mineralization of soil samples and the loss of carbon content, the runoff samples were immediately weighed and dried at 45 °C (Walkley and Black 1934), and the dried sediment was used to calculate the soil loss rate. The second set of runoff samples with sediment was collected at 10 min intervals in the same manner as the first set of samples and was sieved through 5, 2, 1, 0.5, and 0.25 mm screen openings. Sediment fractions remaining on the sieves and material that passed through the 0.25 mm sieve were dried and weighed. During each experiment, velocities of sheet flow and rill concentrated flow were measured with a dye tracing method.

2.4 Analytical methods and computation

The average runoff rate and soil loss rate were the mean of the entire experimental process for each run. The methods of mean weight diameter, MWD (Bavel 1949), and geometric mean diameter, GMD (Mazurak 1950; Gardner 1956), were

used to represent soil aggregate size distribution. The MWD and GMD are defined using Eq. (1) and (2):

$$\text{MWD} = \sum_{i=1}^n x_i y_i \quad (1)$$

$$\text{GMD} = \exp \left[\frac{\left(\sum_{i=1}^n w_i \ln x_i \right)}{\left(\sum_{i=1}^n w_i \right)} \right] \quad (2)$$

where x_i is the mean diameter of each size class, y_i is the proportion of each size class with respect to the total sample, and w_i is the weight of each size class.

The first set of dried sediment samples was used to analyse the SOC concentration, and the second set of dried sediment fractions was used to measure aggregate organic carbon content (Walkley and Black 1934). The enrichment ratio (ER_{SOC}), as defined by Massey and Jackson (1952), is the ratio of organic carbon content in eroded sediment to the tested soil organic carbon. The SOC cementing agent index was aggregate stability (MWD) divided by the SOC content (%), which was considered the quality of the SOC cementing agent for soil aggregate stability.

Statistical data analysis was performed using the software package Excel (2003) and the SPSS 23.0. ANOVA was used to detect the effects of sheet erosion and rill erosion treatments and rainfall intensity. For the results of multiple comparisons, the method of least significant difference (LSD) was used, and the values were statistically significant at $P < 0.05$.

3 Results

3.1 Runoff and soil loss

Runoff from the sheet and rill erosion dominated treatments showed no significant difference under the same rainfall intensity (Table 1). However, under rainfall intensities of 50 and 100 mm h⁻¹, soil loss from the RED treatment was 1.4 and 3.5 times higher, respectively, than those from the SED treatment, and the sediment concentration was 1.3 and 1.4 times greater, respectively, than that from the SED treatment. When the rainfall intensity increased from 50 to 100 mm h⁻¹, the runoff increased by 2.4 times on average, and soil loss increased greatly by 17.6 times for the RED treatment and by 7.1 times for the SED treatment. Statistical analysis revealed significant effects of sheet and rill erosion treatments and rainfall intensities on the soil loss and sediment concentration ($P < 0.05$).

3.2 Soil aggregate loss

3.2.1 Sediment aggregate size distributions

The proportion of 0–0.25 mm aggregates in the tested soil was the largest among the six aggregate fractions, which occupied

45.8% (Table 2) of the total aggregate content. For the SED treatment, the proportion of 0–0.25 mm aggregates in the eroded sediment was lower than that in the tested soil under 50 mm h⁻¹ rainfall intensity and accounted for 41.1% of the total aggregate content; however, under 100 mm h⁻¹ rainfall intensity, the proportion was larger than that in the tested soil and occupied 73.1% of the total aggregate content. For the RED treatment, the proportion of 0–0.25 mm aggregates in the sediment was smaller than that in the tested soil under both rainfall intensities of 50 and 100 mm h⁻¹ and accounted for 32.7 and 36.8%, respectively. Moreover, compared with the tested soil, the proportions of 0.25–0.5 and > 5 mm aggregates in the sediment decreased for both treatments under the two rainfall intensities, whereas those of the 1–2 and 2.5 mm aggregate increased. Furthermore, compared with the tested soil, the proportion of 0.5–1 mm aggregates in the sediment showed three trends, i.e. an increasing trend for both treatments under 50 mm h⁻¹ rainfall intensity, a decreasing trend for the SED treatment under 100 mm h⁻¹ rainfall intensity and being more or less for the RED treatment under 100 mm h⁻¹ rainfall intensity. When the rainfall intensity increased from 50 to 100 mm h⁻¹, except for the proportions of 0–0.25 and > 5 mm aggregates were increased, other aggregate fractions decreased for both treatments.

To further illustrate the soil aggregate size distribution characteristics, the indicators MWD and GMD were used (Table 2). Compared with the tested soil, both the MWD and GMD for the sediment decreased, and the decrements for the SED treatment were higher than those for the RED treatment. As the rainfall intensity increased from 50 to 100 mm h⁻¹, both MWD and GMD for the SED treatment decreased, whereas the values increased for the RED treatment.

3.2.2 Sediment aggregates loss processes

Figure 1 presents the temporal variations for the losses of the six sediment aggregates for the SED and RED treatments. Under rainfall intensities of 50 and 100 mm h⁻¹, the loss rates of the sediment aggregate fractions for the RED treatment showed greatly change with the rainfall duration; however, for the SED treatment, the loss rates peaked at 25 min and then decreased and maintained at steady trend. Moreover, the loss rates of the six aggregate fractions for the SED treatments were all less than those for the RED treatment, and the loss rate variations of the six aggregate fractions were similar for each treatment.

3.3 SOC and aggregate organic carbon losses

3.3.1 SOC loss and the enrichment ratio

SOC losses for the RED treatments were 1.7 and 3.8 times larger than those from the SED treatments under rainfall

Table 1 Runoff, soil loss and sediment concentration for both treatments of sheet erosion and rill erosion dominated

Water erosion pattern	Rainfall intensity (mm h ⁻¹)	Runoff (mm)	Soil loss (g m ⁻²)	Sediment concentration (g L ⁻¹)
Sheet erosion dominated (SED)	50	48.2 ± 4.0 b ^a	64.2 ± 5.0 d	1.3 ± 0.0 d
Rill erosion dominated (RED)		50.9 ± 2.6 b	90.8 ± 23.3 c	1.8 ± 0.5 c
Sheet erosion dominated (SED)	100	114.3 ± 17.8 a	454.2 ± 133.3 b	9.1 ± 0.8 b
Rill erosion dominated (RED)		124.2 ± 13.4 a	1595.8 ± 320.8 a	12.9 ± 1.7 a

^a The number after “±” is the standard deviation (SD); the same letter in the same column is not significantly different at $P < 0.05$ according to LSD tests

intensities of 50 and 100 mm h⁻¹, respectively (Table 3). As the rainfall intensity increased from 50 to 100 mm h⁻¹, SOC loss increased by 7.2 and 16.4 times for the treatments of SED and RED, respectively. However, SOC enrichment ratios (ER_{SOC}) in eroded sediment for the RED treatments were approximately 1, which was 13.4 and 7.3% less than those for the SED treatments under rainfall intensities of 50 and 100 mm h⁻¹, respectively. Statistical analysis revealed significant effects of both sheet erosion and rill erosion patterns on SOC loss and ER_{SOC} ($P < 0.05$). Moreover, rainfall intensity also had significant effects on SOC loss, whereas ER_{SOC} was not significantly affected.

3.3.2 Aggregate organic carbon losses

The organic carbon content of 0–0.25 mm aggregates in the tested soil was the lowest among the six aggregate fractions (Table 4). Compared with the tested soil, the organic carbon content of 0–0.25 mm aggregates in the sediment for the SED treatment increased by 14.89 and 14.29% under rainfall intensities of 50 and 100 mm h⁻¹, respectively, and for the RED treatment, the content increased by 33.33 and 22.08%, respectively. Moreover, when the rainfall intensity increased from 50 to 100 mm h⁻¹, the organic carbon contents of 0.25–0.5, 0.5–1 and 2–5 mm sediment aggregates increased significantly for the SED treatments; whereas the change in organic carbon contents in the other sediment aggregates was not significant. For the RED treatments, the organic carbon contents of 0.25–

0.5, 0.5–1 and > 5 mm aggregates increased significantly when rainfall intensity increased from 50 to 100 mm h⁻¹, but the organic carbon contents decreased significantly in the other sediment aggregates.

The aggregate organic carbon loss of each aggregate fraction was calculated by multiplying the organic carbon content of each aggregate fraction by the mass of soil aggregate (Fig. 2). The aggregate organic carbon loss from each aggregate fraction for the RED treatments was significantly higher than that for the SED treatments, except the 0.25–0.5 mm aggregate fraction was significant under the 50 mm h⁻¹ rainfall intensity. When rainfall intensity increased from 50 to 100 mm h⁻¹, aggregate organic carbon loss increased from 1.04 to 5.87 times among the six aggregate fractions for the SED treatment, whereas the lost increased from 3.82 to 27.84 times for the RED treatment (Fig. 2), which implied that sediment aggregate organic carbon loss for the RED was more sensitive to rainfall intensity, compared with the SED treatment.

4 Discussion

4.1 Characterization of soil aggregates loss for sheet and rill erosion

Some studies show that rainfall intensity, slope gradient and original soil aggregate distribution influence the aggregate

Table 2 Aggregate size distributions in sediment and its indicators for both treatments of sheet erosion and rill erosion dominated

Water erosion pattern	Rainfall intensity (mm h ⁻¹)	Aggregate size distributions in sediment (%)						Indicators (mm)	
		0–0.25 mm	0.25–0.5 mm	0.5–1 mm	1–2 mm	2–5 mm	> 5 mm	MWD ^a	GMD ^b
Sheet erosion dominated (SED)	50	41.1	5.4	13.9	17.2	19.0	3.4	1.32	0.74
Rill erosion dominated (RED)		32.7	5.6	10.7	14.2	27.1	9.7	1.82	1.01
Sheet erosion dominated (SED)	100	73.1	3.8	4.1	6.1	8.1	4.8	0.84	0.42
Rill erosion dominated (RED)		36.8	4.4	6.4	11.4	13.6	27.4	2.17	1.09
The tested soil	/	45.8	13.8	6.1	3.0	3.3	28.0	3.03	1.72

^a The MWD is mean weight diameter

^b The GMD is geometric mean diameter

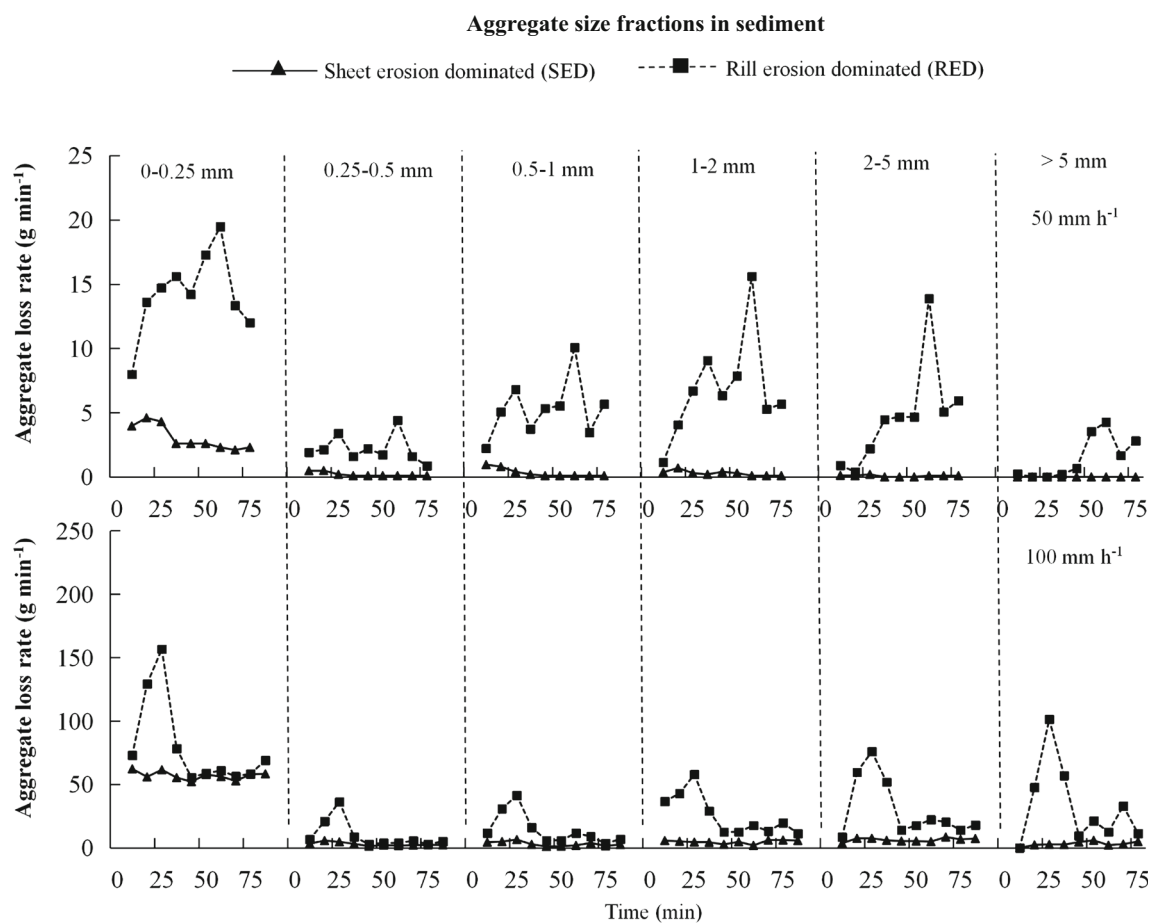


Fig. 1 Temporal variations in sediment aggregate loss rate for both treatments of sheet erosion and rill erosion dominated

transport rate (Loch and Donnollan 1983; Proffitt and Rose 1991; Rose et al. 2007; Asadi et al. 2007b). With the same experimental setting, different soil and aggregate losses for the SED and RED treatments could be attributed to different mechanisms of soil detachment and transport. Moss et al. (1979) note that sediment transport can be divided into suspended, saltation and contact (rolling) loads, each normally broadly associated with particular sediment size ranges. Sheet erosion processes are confined to the soil surface and are strongly influenced by raindrop energy, which causes soil aggregate breakdown to a lower level (Mueller-Nedebock et al. 2016). Then, transport by saltation and sheet flow carries the dispersed soil aggregates (suspended and contact loads) downslope at a steady state (Shi et al. 2012). For the SED treatment, raindrop impact force promoted aggregate breakdown to a lower level, and the surface flow delivered the dispersed soil aggregates. With an increase of rainfall intensity, the raindrop impact force increased, and consequently, the larger-sized aggregates were broken down and transported (Table 2). Many experimental results show that during rainfall-driven erosion, when sheet erosion dominates, sediment is enriched with finer particles at early times because of the limited sediment transport capacity of surface flow until

the rills form (Moss et al. 1979; Proffitt and Rose 1991). Therefore, for the SED treatment, the primary driving forces were raindrop impact and sheet flow on the surface.

Soil erosion was accelerated because the preformed rill channel degraded soil structure and weakened aggregate stability. Additionally, rill erosion processes concentrate more flow in the rill channel that can detach more soil aggregates (Armstrong and Stein 1996; Bryan 2000). During the experiments, concentrated flow velocity in the rill channel (25.8 cm s^{-1}) was approximately two times larger than that of the sheet flow in the SED treatment, which facilitated rill development, and the soil loss in the RED treatment greatly increased. With rill development, rill head-cut migration and sidewall expansion would accelerate rill development with larger-sized aggregates detached and transported, and the results showed that the proportion of macro-aggregates ($> 0.25 \text{ mm}$) were greater than 60% (Table 2).

Sheet erosion selectively transports finer sediment particles, whereas no selectivity occurs in sediment transport when rill channels develop (Proffitt et al. 1993). Although the distributions of other sized aggregates (i.e. 0.25–0.5, 0.5–1, 1–2 and 2–5 mm) in sediments varied and did not exhibit apparent trends, the indicators MWD and GMD reflected the

Table 3 Soil organic carbon (SOC) loss and its enrichment ratio (ER) for both treatments of sheet erosion and rill erosion dominated

Water erosion pattern	Rainfall intensity (mm h ⁻¹)	SOC loss (g h ⁻¹ m ⁻²)	Enrichment ratio (ER _{SOC})
Sheet erosion dominated (SED)	50	0.5 ± 0.1 d ^a	1.19 ± 0.05 a
Rill erosion dominated (RED)		0.9 ± 0.2 c	1.03 ± 0.01 b
Sheet erosion dominated (SED)	100	3.9 ± 0.8 b	1.10 ± 0.04 a
Rill erosion dominated (RED)		14.6 ± 2.1 a	1.02 ± 0.01 b

^a The number after “±” is the standard deviation (SD); the same letter at the same column is not significantly different at $P < 0.05$ according to LSD tests

characterizations caused by the sheet and rill erosion (Table 2). Soils with high MWD and GMD are likely to have increased resistance to soil degradation and erosion (Celik 2005). For the RED treatment, undispersed large aggregate transport was associated with rill head-cut migration and sidewall expansion; thus, eroded sediment showed an integrated structure which could explain the non-selective transportation of different aggregate size fractions in the rill erosion.

Moreover, for this Mollisol, soil organic matter content (23.80 ± 0.17 g kg⁻¹) and well-structured soil aggregation were higher than those of a Loess soil. After wet sieving, the Mollisol contained more 0.25–0.5, 1–2, 2–5 and > 5 mm macro-aggregates than Loess soil; therefore, the soil material losses by sheet and rill erosion for Loess soil are greater than those of the Mollisol (Wu et al. 2012).

4.2 Characterization of soil organic carbon loss for sheet and rill erosion

Available literature generally show that different water erosion patterns cause different SOC losses (Palis et al. 1997; Wan and El-Swaify, 1998; Kirkels et al. 2014). This study indicated that the SOC losses for the RED treatments were higher than those for the SED treatments, and the influence of rainfall intensity on SOC losses was significant. As a selective process, surface runoff preferentially transports the finer sediment particles associated with low bulk density SOC (Lowrance and Richard 1988; Lal 2003). Therefore, eroded sediment has finer-sized fractions than those of the original soil, and the ER_{SOC} is always above 1 (Zhang et al., 2006a, b).

Additionally, different water erosion processes also affect the ER_{SOC}. Some studies show that rill and interrill erosion processes have contrasting effects on ER_{SOC} (Schiettecatte et al. 2008a), because rill erosion is less selective or non-selective after a specific critical flow shear stress was exceeded (Wan and El-Swaify, 1998). Zheng et al. (2005) noted that, in the ephemeral gully erosion dominated zone, the ER_{SOC} in eroded sediment initially decreases and then increases with an increase in sediment concentration. Similarly, sediment from the rill channel was also unsorted, and therefore, the ER_{SOC} was approximately 1 and significantly lower than that of sheet erosion (Table 3).

Schiettecatte et al. (2008a) note that the enrichment process is not influenced by raindrop impact when soil aggregate stability is low or SOC within the different soil aggregate classes is equally distributed. Similarly, this study also showed that the ER_{SOC} was not significantly different at rainfall intensities of 50 and 100 mm h⁻¹ either in the SED or RED treatment, which could be explained by “aggregate stripping” with the SOC equally distributed within the different soil aggregate fractions.

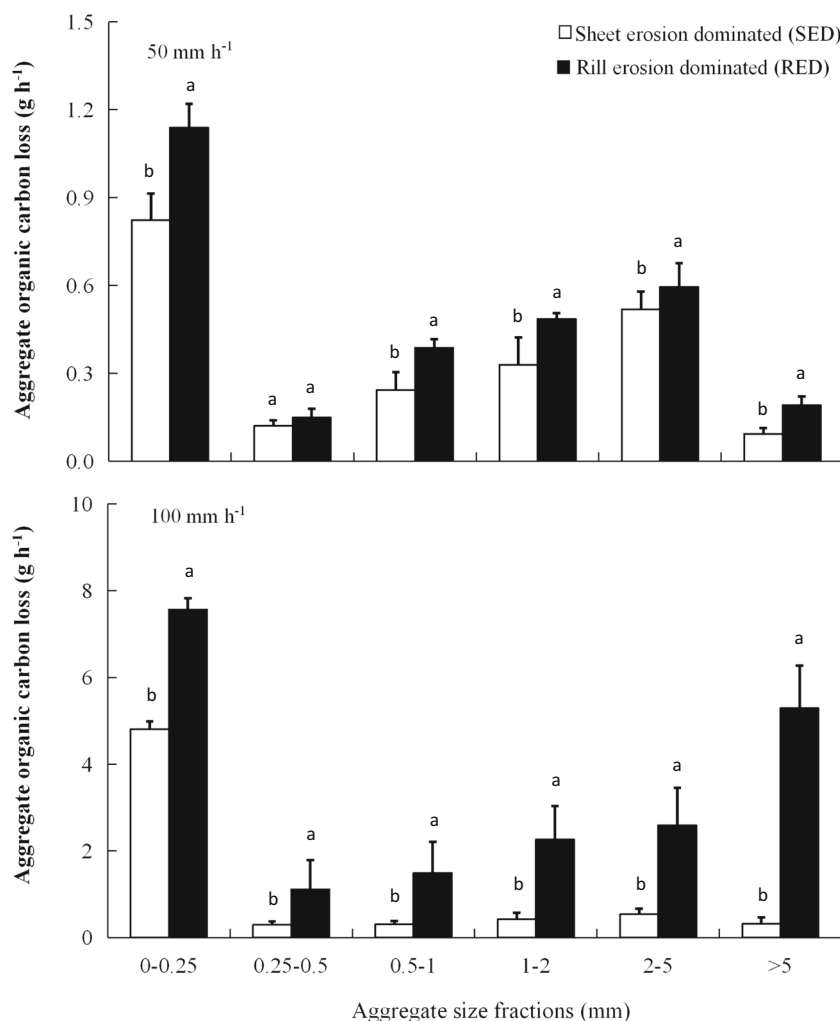
Tisdall and Oades (1982) note that water stable aggregates > 2 mm in diameter in soil with high organic carbon content consist of aggregates and particles held together primarily by a fine network of roots and hyphae. Additionally, Six et al. (2000) note that the soil particles in large aggregates are of low stability and persistence because they are weakly cemented by organic matter. The aggregate changes (Figs. 1 and 2) might be explained by the aggregate properties. Macro-aggregates (> 0.25 mm) might include particulate, non-

Table 4 Aggregate organic carbon contents for both treatments of sheet erosion and rill erosion dominated

Water erosion pattern	Rainfall intensity (mm h ⁻¹)	Aggregate organic carbon contents in sediment (g kg ⁻¹)					
		0–0.25 mm	0.25–0.5 mm	0.5–1 mm	1–2 mm	2–5 mm	> 5 mm
Sheet erosion dominated (SED)	50	14.1 ± 1.4 b ^a	14.0 ± 0.9 a	14.2 ± 1.0 a	14.4 ± 2.8 a	13.9 ± 3.0 a	13.8 ± 3.6 a
Rill erosion dominated (RED)		18.0 ± 1.8 d	15.3 ± 4.4 b	16.2 ± 0.7 c	16.5 ± 0.8 b	15.7 ± 0.9 b	14.0 ± 1.0 a
Sheet erosion dominated (SED)	100	14.0 ± 0.2 b	16.4 ± 2.3 c	16.0 ± 0.2 c	14.7 ± 3.0 a	14.1 ± 2.1 a	14.0 ± 0.8 a
Rill erosion dominated (RED)		15.4 ± 1.0 c	19.1 ± 2.0 d	17.3 ± 0.5 d	14.9 ± 0.8 a	14.3 ± 3.5 a	14.5 ± 2.4 b
The tested soil	/	12.0 ± 0.5 a	15.4 ± 0.2 b	15.1 ± 0.6 b	14.3 ± 0.2 a	14.0 ± 0.1 a	13.6 ± 0.6 a

^a The number after “±” is the standard deviation (SD); the same letter at the same column is not significantly different at $P < 0.05$ according to LSD tests

Fig. 2 Aggregate associated organic carbon loss for both treatments of sheet erosion and rill erosion dominated. Note The same letter at the same aggregate size fraction is not significantly different at $P < 0.05$ according to LSD tests



decomposed and raw organic matter that could be breakdown and dissolved easily by water; thus, the amount of aggregate organic carbon loss showed the greatest discrepancy between the SED and RED treatments (Fig. 2). For the micro-aggregates (< 0.25 mm), the primary components are colloidal humic-type substances and stable clay-mineral complexes. As shown in the time series (Fig. 1), the micro-aggregates (< 0.25 mm) accumulated constantly, and the organic carbon content was stable (Table 4).

Table 5 shows the SOC cementing agent index, which revealed the relationship between SOC content and soil aggregate stability. The physical protection of SOC afforded by aggregation is removed by water erosion when disruptive energy of forces (such as raindrop impact, the shear stress of flowing water and collision with other aggregates) are applied to soil (Lal 2003). Then, aggregates are broken down and labile SOC fractions are released. Therefore, the SOC cementing agent indexes all decrease compared with those of the test soil (Wagner et al. 2007). The processes of disaggregation expose previously protected aggregate organic carbon, which can be transported by surface runoff downward to

lower horizons (Janeau et al. 2014; Ma et al. 2014). In this study, in addition to the above-mentioned mechanism, SOC cementing agent indexes for the RED treatment were all larger than those for the SED treatment at the same rainfall intensity (Table 5), particularly under 100 mm h^{-1} rainfall intensity. These results indicate that different erosion patterns could affect the disaggregation processes, and might further influence

Table 5 Sediment soil organic carbon (SOC) content and its cementing agent index for both treatments of sheet erosion and rill erosion dominated

Water erosion pattern	Rainfall intensity (mm h ⁻¹)	SOC content (%)	SOC cementing agent index (mm)
Sheet erosion dominated (SED)	50	1.30	101.69
Rill erosion dominated (RED)		1.65	110.17
Sheet erosion dominated (SED)	100	1.43	58.70
Rill erosion dominated (RED)		1.52	142.31
The tested soil	/	1.38	219.48

the aggregate organic carbon contents in eroded sediment (Table 4).

Hemelryck et al. (2010) concludes that rapid wetting (slaking) treatment mainly results in a strong reduction of macro-aggregates concomitant with an increase in micro-aggregates, but SOC content in aggregates > 0.25 mm was reduced in slaking samples. In the Mollisol region of Northeast China, the mechanisms of aggregate breakdown by water erosion include slaking (rapid wetting) and macro-cracking (slow wetting) (Le Bissonnais 1996; Le Bissonnais and Arrouays 1997; Wang et al. 2013), which might explain why the aggregate organic carbon contents in sediment of each fraction from the RED treatment (slow wetting) were higher than those from the SED treatment (rapid wetting). Moreover, Six et al. (1999, 2004) also found that larger aggregates are less persistent than small aggregates and are prone to breakdown and varied under different agricultural practices, and water erosion processes, among others. Huang et al. (2010) also noted that, in slightly and moderately eroded Ultisols, the contents of organic carbon in aggregate fractions are higher than those in severely eroded Ultisols. Thus, redistribution of aggregate organic carbon content in sediments from different water erosion patterns also varies, with similar results also found by Hemelryck et al. (2010).

5 Conclusions

In this study, the effects of sheet and rill erosion on soil aggregates and SOC losses were experimentally quantified. Sheet and rill erosion produced different amounts of eroded soil material with different degrees of aggregation, and caused distinguishing characteristics of SOC and aggregate organic carbon loss. Both of soil and SOC losses from the RED treatment were significantly higher than those from SED treatment. As the rainfall intensity increased from 50 to 100 mm h⁻¹, soil and SOC losses increased by 7.1 and 7.2 times for the SED treatment, whereas those for the RED treatment increased by 17.6 and 16.4 times, respectively. The SOC enrichment ratios, although not significant, in eroded sediment caused by the RED treatment were approximately 1, which was 13.4 and 7.3% less than those caused by the SED treatment. The sediment aggregate size redistribution showed that 73.1% of the loss of aggregates was from micro-aggregates (< 0.25 mm) for the SED treatment, whereas macro-aggregates (> 0.25 mm) were the primary materials lost for the RED treatment, which occupied 65.2% in the total aggregate contents. Compared with the tested soil, the organic carbon contents of 0–0.25 mm aggregates in sediment increased from 14.3 to 33.3% for both SED and RED treatments under rainfall intensities of 50 and 100 mm h⁻¹. These results showed that the different mechanisms of aggregate breakdown and transport by sheet and rill erosion could affect the

aggregate organic carbon content. Therefore, in further study, the erosion pattern could be used as one factor in modelling erosion-induced SOC dynamics for agricultural ecosystem carbon flux.

Acknowledgements We appreciate the suggestions of the anonymous reviewers and the editor.

Funding information This study was funded by the National Key R&D Program of China (Grant number 2016YFE0202900), and the National Natural Science Foundation of China (Grant No. 41571263).

References

- An J, Zheng FL, Lu J, Li GF (2012) Investigating the role of raindrop impact on hydrodynamic mechanism of soil erosion under simulated rainfall conditions. *Soil Sci* 177(8):517–526. <https://doi.org/10.1097/SS.0b013e3182639de1>
- Armstrong SM, Stein OR (1996) Eroded aggregate size distributions from disturbed lands. *Trans ASAE* 39:137–143
- Asadi H, Ghadiri H, Rose CW, Yu B, Hussein J (2007) An investigation of flow-driven soil erosion processes at low streampowers. *J Hydrol* 342:134–142. <https://doi.org/10.1016/j.jhydrol.2007.05.019>
- Bajracharya RM, Lal R, Kimble JM (2000) Diurnal and seasonal CO₂-C flux from soil as related to erosion phases in central Ohio. *Soil Sci Soc Am J* 64:286–293. <https://doi.org/10.2136/sssaj2000.641286x>
- Bavel CHMV (1949) Mean weight-diameter of soil aggregates as a statistical index of aggregation. *Soil Sci Soc Am J* 14:20–23
- Bryan RB (2000) Soil erodibility and processes of water erosion on hill-slope. *Geomorphology* 32:385–415. [https://doi.org/10.1016/S0169-555X\(99\)00105-1](https://doi.org/10.1016/S0169-555X(99)00105-1)
- Celik I (2005) Land-use effects on organic matter and physical properties of soil in a southern Mediterranean highland of Turkey. *Soil Till Res* 83:270–277. <https://doi.org/10.1016/j.still.2004.08.001>
- Cheng SL, Fang HJ, Zhu TH, Zheng JJ, Yang XM, Zhang XP, Yu GR (2010) Effects of soil erosion and deposition on soil organic carbon dynamics at a sloping field in Black Soil region, Northeast China. *Soil Sci Plant Nutr* 56:521–529. <https://doi.org/10.1111/j.1747-0765.2010.00492.x>
- Foster GR, Wischmeier WH (1974) Evaluating irregular slopes for soil loss prediction. *Trans ASAE* 17:305–309
- Gardner WR (1956) Representation of soil aggregate-size distribution by a logarithmic-normal distribution. *Soil Sci Soc Am J* 20:151–153. <https://doi.org/10.2136/sssaj1956.03615995002000020003x>
- Hemelryck HV, Fiener P, Van Oost K, Govers G, Merckx R (2010) The effect of soil redistribution on soil organic carbon: an experimental study. *Biogeosciences* 7:3971–3986. <https://doi.org/10.5194/bg-7-3971-2010>
- Huang L, Wang CY, Tan WF, Hu HQ, Cai CF, Wang MK (2010) Distribution of organic matter in aggregates of eroded Ultisols, Central China. *Soil Till Res* 108:59–67. <https://doi.org/10.1016/j.still.2010.03.003>
- Janeau JL, Gillard LC, Grellier S, Jouquet P, Le Thi PQ, Luu TNM, Ngo QA, Orange D, Pham DR, Tran DT, Tran SH, Trinh AD, Valentin C, Rochelle-Newall E (2014) Soil erosion, dissolved organic carbon and nutrient losses under different land use systems in a small catchment in northern Vietnam. *Agr Water Manage* 146:314–323. <https://doi.org/10.1016/j.agwat.2014.09.006>
- Jin K, Comelis WM, Gabriels D, Baert M, Wu HJ, Schiettecatte W, Cai DX, De NS, Jin JY, Hartmann R, Hofman G (2009) Residue cover and rainfall intensity effects on runoff soil organic carbon losses. *Catena* 78:81–86. <https://doi.org/10.1016/j.catena.2009.03.001>

- Kirkels FMSA, Cammeraat LH, Kuhn NJ (2014) The fate of soil organic carbon upon erosion, transport and deposition in agricultural landscapes—a review of different concepts. *Geomorphology* 226:94–105. <https://doi.org/10.1016/j.geomorph.2014.07.023>
- Kisic I, Basic F, Nestroy O, Mesic M, Butorac A (2002) Chemical properties of eroded soil material. *J Agron Crop Sci* 188:323–334. <https://doi.org/10.1046/j.1439-037X.2002.00571.x>
- Kuhn NJ, Hoffmann T, Schwanghart W, Dotterweich M (2009) Agricultural soil erosion and global carbon cycle: controversy over? *Earth Surf Process Landf* 34:1033–1038
- Lal R (1976) Soil erosion problems on Alfisols in western Nigeria and their control. IITA, Monograph 1, Ibandan, Nigeria, p 208
- Lal R (2003) Soil erosion and the global carbon budget. *Environ Int* 29: 437–450. [https://doi.org/10.1016/S0160-4120\(02\)00192-7](https://doi.org/10.1016/S0160-4120(02)00192-7)
- Le Bissonnais Y (1996) Aggregate stability and assessment of soil crustability and erodibility. 1. Theory and methodology. *Eur J Soil Sci* 47:25–437
- Le Bissonnais Y, Arrouays D (1997) Aggregate stability and assessment of soil crustability and erodibility. 2. Application to humic loamy soils with various organic carbon contents. *Eur J Soil Sci* 48:39–48. <https://doi.org/10.1111/j.1365-2389.1997.tb00183.x>
- Liu G, Xiao H, Liu PL, Zhang Q, Zhang JQ (2016) An improved method for tracing soil erosion using rare earth elements. *J Sediment Res* 16: 1670–1679
- Loch RJ, Donnollan TE (1983) Field rainfall simulator studies on two clay soils of the darling downs, Queensland. II. Aggregate breakdown, sediment properties and soil erodibility. *Aus J Soil Res* 47: 107–111
- Lowrance R, Richard RG (1988) Carbon movement in runoff and erosion under simulated rainfall conditions. *Soil Sci Soc Am J* 52:1445–1448. <https://doi.org/10.2136/sssaj1988.03615995005200050045x>
- Ma W, Li Z, Ding K, Huang J, Nie X, Zeng G, Wang S, Liu G (2014) Effect of soil erosion on dissolved organic carbon redistribution in subtropical red soil under rainfall simulation. *Geomorphology* 226: 217–225. <https://doi.org/10.1016/j.geomorph.2014.08.017>
- Maïga-Yaleu S, Guiguemde I, Yacouba H, Karambiri H, Ribolzi O, Bary A, Ouedraogo R, Chaplot V (2013) Soil crusting impact on soil organic carbon losses by water erosion. *Catena* 107:26–34. <https://doi.org/10.1016/j.catena.2013.03.006>
- Massey HF, Jackson ML (1952) Selective erosion of soil fertility constituents. *Soil Sci Soc Am J* 16:353–356. <https://doi.org/10.2136/sssaj1952.03615995001600040008x>
- Mazurak AP (1950) Effect of gaseous phase on water-stable synthetic aggregate. *Soil Sci* 69:135–148. <https://doi.org/10.1097/00010694-195002000-00005>
- Ministry of Water Resources, Chinese Academy of Sciences, Chinese Academy of Engineering (2010) Soil loss control and ecological security in China: the northeast black soil volume. The Science Press, Beijing, pp 41–55, 209–230 (in Chinese)
- Morgan PRC (2005) Soil erosion and conservation, 3rd edn. Blackwell Publishing, Oxford, p 304
- Moss AJ, Walker PH, Hutka J (1979) Raindrop-stimulated transportation in shallow water flows: an experimental study. *Sediment Geol* 22: 165–184. [https://doi.org/10.1016/0037-0738\(79\)90051-4](https://doi.org/10.1016/0037-0738(79)90051-4)
- Mueller-Nedebock D, Chivenge P, Chaplot V (2016) Selective organic carbon losses from soils by sheet erosion and main controls. *Earth Surf Process Landform* 41:1399–1408
- Nadeu E, de Vente J, Martinez-Mena M, Boix-Fayos C (2011) Exploring particle size distribution and organic carbons pools mobilized by different erosion processes at the catchment scales. *J Soils Sediments* 11:667–678. <https://doi.org/10.1007/s11368-011-0348-1>
- Palis RG, Ghandiri H, Rose CW, Saffigna PG (1997) Soil erosion and nutrient loss. 3. Changes in the enrichment ratio of total nitrogen and organic carbon under rainfall detachment and entrainment. *Aust J Soil Res* 35:891–905. <https://doi.org/10.1071/S92060>
- Polyakov VO, Lal R (2004) Soil erosion and carbon dynamics under simulated rainfall. *Soil Sci* 169:590–599. <https://doi.org/10.1097/01.ss.0000138414.84427.40>
- Proffitt APB, Rose CW (1991) Soil erosion processes: II. Settling velocity characteristics of eroded sediment. *Aust J Soil Res* 29:685–695. <https://doi.org/10.1071/SR9910685>
- Proffitt APB, Rose CW, Lovell CJ (1993) Settling velocity characteristic of sediment detached from a soil surface by raindrop impact. *Catena* 20:27–40. [https://doi.org/10.1016/0341-8162\(93\)90027-M](https://doi.org/10.1016/0341-8162(93)90027-M)
- Puustinen M, Koskiaho J, Peltonen K (2005) Influence of cultivation methods on suspended solids and phosphorus concentrations in surface runoff on clayey sloped fields in boreal climate. *Agric Eco Environ* 105:565–579. <https://doi.org/10.1016/j.agee.2004.08.005>
- Rose CW, Yu B, Ghadiri H, Asadi H, Parlange JY, Hogarth WL, Hussein J (2007) Dynamic erosion of soil in steady sheet flow. *J Hydrol* 333: 449–458. <https://doi.org/10.1016/j.jhydrol.2006.09.016>
- Rozañov BG, Targulian V, Orlov DS, Turner BL, Clark WC, Kates RW, Richards JF, Mathews JT, Meyer WB (1993) The earth as transformed by humans action: global and regional changes in the biosphere over the past 300 years. Cambridge University Press, Cambridge, pp 203–214
- Schiettecatte W, Gabriels D, Cornelis WM, Hofman G (2008a) Enrichment of organic carbon in sediment transport by interrill and rill erosion processes. *Soil Sci Soc Am J* 72:50–55
- Schiettecatte W, Gabriels D, Cornelis WM, Hofman G (2008b) Impact of deposition on the enrichment of organic carbon in eroded sediment. *Catena* 72:340–347
- Schimel DS, House JI, Hibbard KA (2001) Recent patterns and mechanisms of carbon exchange by terrestrial ecosystems. *Nature* 414: 169–172. <https://doi.org/10.1038/35102500>
- Shi ZH, Fang NF, Wu FZ, Wang L, Yue BJ, Wu GL (2012) Soil erosion processes and sediment sorting associated with transport mechanisms on steep slopes. *J Hydrol* 454:123–130
- Six J, Bossuyt H, Degryze S, Denef K (2004) A history of research on the link between (micro)aggregates, soil biota, and soil organic matter dynamics. *Soil Till Res* 79:7–31. <https://doi.org/10.1016/j.still.2004.03.008>
- Six J, Elliott ET, Paustian K (1999) Aggregate and soil organic matter dynamics under conventional and no-tillage systems. *Soil Sci Soc Am J* 63:1350–1358. <https://doi.org/10.2136/sssaj1999.6351350x>
- Six J, Paustian K, Elliott ET, Combrink C (2000) Soil structure and organic matter: I Distribution of aggregate-size classes and aggregate-associated carbon. *Soil Sci Soc Am J* 64:681–689. <https://doi.org/10.2136/sssaj2000.642681x>
- Stallard RF (1998) Terrestrial sedimentation and the carbon cycle: coupling weathering and erosion to carbon burial. *Glob Biogeochem Cycles* 12:231–257. <https://doi.org/10.1029/98GB00741>
- Starr GC, Lal R, Malone R, Hothem D, Owens L, Kimble J (2000) Modeling soil carbon transported by water erosion processes. *Land Degrad Devel* 11:83–91. [https://doi.org/10.1002/\(SICI\)1099-145X\(200001/02\)11:1<83::AID-LDR370>3.0.CO;2-W](https://doi.org/10.1002/(SICI)1099-145X(200001/02)11:1<83::AID-LDR370>3.0.CO;2-W)
- Sutherland RA, Watung RL, El-Swaify SA (1996) Splash transport of organic carbon and associated concentration and mass enrichment ratios for an Oxisol, Hawai'i. *Earth Surf Process Landform* 21: 1145–1162. [https://doi.org/10.1002/\(SICI\)1096-9837\(199612\)21:12<1145::AID-ESP657>3.0.CO;2-H](https://doi.org/10.1002/(SICI)1096-9837(199612)21:12<1145::AID-ESP657>3.0.CO;2-H)
- Tans PP, Fung IY, Takahashi T (1990) Observational constraints on the global atmospheric CO₂ budget. *Science* 247:1431–1438. <https://doi.org/10.1126/science.247.4949.1431>
- Tiessen H, Stewart JWB, Betany JR (1982) Cultivation effects on the amount and concentration of carbon, nitrogen and phosphorus in grassland soils. *Agron J* 74:831–834. <https://doi.org/10.2134/agronj1982.00021962007400050015x>
- Tisdall JM, Oades JM (1982) Organic matter and water stable aggregates in soils. *Soil Sci* 33:141–163

- Van Oost K, Quine TA, Govers G (2007) The impact of agricultural soil erosion on the global carbon cycle. *Science* 318:626–629. <https://doi.org/10.1126/science.1145724>
- Wagner S, Cattle SR, Scholten T (2007) Soil-aggregate formation as influenced by clay content and organic-matter amendment. *Soil Sci Plant Nutr* 170:173–180
- Walkley A, Black IA (1934) An examination of the Degtjareff method for determining soil organic matter and a proposed modification of the chromic acid titration method. *Soil Sci* 37:29–38. <https://doi.org/10.1097/00010694-193401000-00003>
- Wan Y, El-Swaify SA (1998) Characterizing interrill sediment size by partitioning splash and wash processes. *Soil Sci Soc Am J* 62:430–437. <https://doi.org/10.2136/sssaj1998.03615995006200020020x>
- Wang B, Zheng FL, Romkens M, Darboux F (2013) Soil erodibility for water erosion: a perspective and Chinese experiences. *Geomorphology* 187: 1–10. <https://doi.org/10.1016/j.geomorph.2013.01.018>
- Wang WJ, Zhang SW, Deng RX (2011) Gully status and relationship with landscape pattern in black soil area of Northeast China. *Trans Chin Soc Agri Eng* 27:192–198 (in Chinese)
- Wang X, Cammeraat ELH, Cerli C, Kalbitz K (2014) Soil aggregation and the stabilization of organic carbon as affected by erosion and deposition. *Soil Biol Biochem* 72:55–65. <https://doi.org/10.1016/j.soilbio.2014.01.018>
- Wei JB, Xiao DN (2005) Landscape pattern and its functioning after ecological reconstruction in black soil region of northeast China. *Chin J Appl Ecol* 16:1699–1705 (in Chinese)
- Wu FZ, Shi ZH, Yue BJ, Wang L (2012) Particle characteristics of sediment in erosion on hillslope. *Acta Pedol Sin* 49(06):1235–1240 (in Chinese)
- Young RA, Onstad CA (1982) Erosion characteristics of three northwest soils. *Trans ASAE* 25(2):366–371
- Zhang JH, Quine TA, Ni SJ, Ge FL (2006a) Stocks and dynamics of SOC in relation to soil redistribution by water and tillage erosion. *Glob Chang Biol* 12:1834–1841
- Zhang XP, Liang AZ, Shen Y (2006b) Erosion characteristics of black soils in Northeast China. *Sci Geogr Sin* 26:687–692 (in Chinese)
- Zheng FL, He XB, Gao XT, Zhang C, Tang KL (2005) Effects of erosion patterns on nutrient loss following deforestation on the Loess Plateau of China. *Agric Eco Environ* 108:85–97. <https://doi.org/10.1016/j.agee.2004.12.009>
- Zhou PH, Zhang XD, Tang KL (2000) Simulation test hall rainfall device State Key Laboratory of soil erosion in Loess Plateau soil erosion and dryland agriculture. *Bull Soil Water Cons* 20:27–30 (in Chinese)